Multi-object Tracking Based on Particle Probability Hypothesis Density Tracker in Microscopic video

Chunmei Shi*, Lingling Zhao†, Peijun Ma†, Xiaohong Su†, Junjie Wang† and Chiping Zhang*
*Department of Mathematics, Harbin Institute of Technology,Harbin 150001, China
Email: shichunmei1210@gmail.com
†School of Computer Science and Technology, Harbin Institute of Technology, Harbin 150001, China

***Abstract*—Research on biological objects requires tracking hundreds of micro-objects from the microscopy video. We propose an automated tracking framework to extract trajectories of micro-objects. This framework uses a particle probability hypothesis density (PF-PHD) tracker to implement a recursive Bayesian state estimation and trajectories association. In the framework, an ellipse target model is presented to describe the micro-objects with shape parameters instead of point-like targets. Furthermore, an orientation and positional constraint model is developed to deal with the data association of crossing trajectories in multitarget tracking. Using this framework, a significantly larger number of tracks are obtained than manual tracking. The experiments on simulated image sequences of microtubule movement are performed in order to evaluate the proposed PF-PHD tracking method.**

I. Introduction

At present, a considerable part of research on biological dynamics is shifting towards detecting and tracking micro-objects (cells, bacteria, infecting viruses, etc) of microscopy images, allowing the visualization of specific biological processes in real time and in two dimensions or three dimensions[1], [2], [3]. With these exciting developments [4], [5], [6], biologists are now able to obtain a real time view of activities in micro-objects, like filming cells and documenting the infectious disease processes in living systems. Despite significant technical advances in tracking moving objects, micro-object tracking remains a challenging task due to the complex nature of biological applications. Microscopic sequences are usually populated with visually similar tiny structures that have intricate motion patterns and sophisticated interactions with other structures such as birth and merging. Moreover, the micro-objects may enter, exit, disappear from the field of view or be occluded by other cellular objects. In addition some microscopy images have sequences that are contaminated with high levels of noise which complicates detection. Therefore, it is important to track of multiple micro-objects in an automatic, reproducible, and unprejudiced manner.

For decades, there have been many ways and methods for micro-objects tracking. For a general summary of object tracking methods we refer to [7], [8], [9]. The simplest way besides manual segmentation is thresholding. Thresholding might be applicable when the objects have sufficiently and consistently different intensities compared to their background. However, it will fail in the case of severe noise, poor contrast.

There is a kind of method that performs cell tracking using the energy function [10]. The level set method is an example that can be used to tackle object topology changes and generate a segmentation of the object [11], [12]. Unfortunately, the close proximity of cells and the occlusion in the microscopy videos make cell tracking difficult. Active contour approaches an energy depending on the segmentation curve, where a low energy corresponds to a curve with the desired properties [1], [13]. Typically, these methods are driven by the data in some feature space and make a regularity assumption on the smoothness of the curve.

The target tracking approaches based on nearest neighbor and smooth-motion criteria [14], [15] are applicable to image data showing limited numbers of clearly distinguishable spots against relatively backgrounds, but fail to yield reliable results in the case of poor imaging conditions. Methods based on minimal cost path searching [16], [17], [18] have also been proposed. However, these have been demonstrated to work well only for a single object or a very limited number of well-separated objects.

Another common approach to dealing with microscopic target tracking is by using a multiple hypothesis tracking (MHT) [19] and joint probabilistic data association (JPDA) filter [20]. Motion filters with prior knowledge in the time domain, such as Kalman filter (KF) [21] and particle filter (PF) [20], are applied to seek an approximate globally optimal solution in space, similar to JPDA but capable of adaptively dealing with the birth and death of particle trajectories in biological application. The critical factors in these approaches are reliable motion models and corresponding data association for the motion parameter update.

In recent years, Mahler devised the probability hypothesis density (PHD) filter as a first order statistic of the multitarget filter [22]. Due to its good performance and significantly low processing time, the filter has been recently used in various applications [23], [24]. In biological applications, Gaussian-Mixture PHD filter was developed on microscopic visual data to extract trajectories of free-swimming bacteria in order to analyze their motion [6]. Further, the point-like target model usually ignores many important geometric shape features for most biological micro-objects with various shapes. Therefore, these approaches can hardly be extended to the complicated real biological scenarios.

Over time in the microscopy image sequences, some of micro-objects may disappear; new micro-objects may appear;

978-1-4799-7502-0/14 $31.00 © 2014 IEEE
DOI 10.1109/BIBE.2014.24

and the surviving micro-objects may evolve to new states based on their dynamics. Moreover, due to microscopy limitations, only some objects are detected at each frame and many measurements are spurious detections (clutter). PHD filter can effectively deal with such biological cases. In this paper, we propose a framework for the automatic detection and tracking of biological micro-objects in microscopy images by considering geometric shape features and dynamic. We use mathematical morphology (MM) to enhance image quality and extract the shape parameters as the measurement information in the next tracker. Then, we use a particle filter PHD (PF-PHD) tracker to allow an implementation for target initialization, state estimation, and track continuity.

The contributions of this paper include the following.

1) We propose a complete Bayesian filter framework using particle-PHD filter for the automatic detection and tracking of biological micro-objects in microscopy images.
2) A target shape model is presented to describe the micro-objects of interest not only with their centroid but also with structure parameters. The model can enable the calculation of area and shape of the micro-objects instead of point-like targets.
3) An orientational and positional constraint model is proposed in the track continuity to handle the issue of crossing trajectories.

The remainder of the paper is organized as follows. In Section II, we give the background information of the PHD filter. The PF-PHD tracking framework is provided in Section III. The experimental results of applying PF-PHD tracker to microscopy images sequences are presented in Section IV. Section V concludes.

II. Background of PHD filter

Mahler proposed random finite sets (RFS) as a theoretical framework for multitarget data fusion [25]. In random set theory, let $\mathbf{x}_1, \ldots, \mathbf{x}_{N_t}$ and $\mathbf{y}_1, \ldots, \mathbf{y}_{M_t}$ be the states of all N_t targets and all M_t measurements at time t, respectively. We can describe each time by two RFSs: $X_t = \{\mathbf{x}_1, \ldots, \mathbf{x}_{N_t}\}$ for states and $Y_t = \{\mathbf{y}_1, \ldots, \mathbf{y}_{M_t}\}$ for measurements.

In the RFS based Bayesian tracking approach, the goal is to estimate the joint multitarget posterior density of the states at each time step t using the set of all measurements up to this time step. This posterior density $p_t(X_t|Y_{1:t})$, can be described by a discrete probability distribution and a joint probability density on the targets' cardinality and state [26], respectively. The general theoretically optimal approach to multitarget tracking is the recursive Bayesian filter (1) as follows:

$$\begin{aligned} p_{t|t-1}(X_t|Y_{1:t-1}) &= \int f_{t|t-1}(X_t|X)p_{t-1}(X|Y_{1:t-1})\mu_s(dX) \\ p_t(X_t|Y_{1:t}) &= \frac{g_t(Y_t|X_t)p_{t|t-1}(X_t|Y_{1:t-1})}{\int g_t(Y_t|X)p_{t|t-1}(X|Y_{1:t-1})\mu_s(dX)} \end{aligned} \quad (1)$$

where μ_s is some reference measure on the space of finite subsets of $\mathcal{X}$ [26]. The Bayesian filtering framework is used to recursively estimate this combinational posterior density using multitarget transition density $f_{t|t-1}(X_t|X_{t-1})$ and measurement likelihood $g_t(Y_t|X_t)$. Although the filter provides an elegant Bayesian formulation of the multitarget filtering problem, it is computationally intractable. To overcome this problem, Mahler [25] proposed to propagate the probability hypothesis density (PHD), or posterior intensity $D_{t|t}(x)$ which is the first statistical moment of the probability density function $p_t(X_t|Y_{1:t})$. The integral of the PHD over a region in a state space is the expected number of targets within this region. Consequently, the peaks of PHD are the states with the highest local concentration and that can be used to generate the estimates for states of targets. It has been shown that this posterior intensity PHD can be calculated using the following recursive equations. The PHD prediction equation is

$$D_{t|t-1}(x) = b_t(x) + \int p_S(\zeta)f_{t|t-1}(x|\zeta)D_{t-1|t-1}(\zeta)d\zeta \quad (2)$$

where $b_t(\cdot)$ denotes the intensity function of the random finite set of spontaneous birth targets, and $p_S(\zeta)$ is the survival probability that the target will exist given that it has a previous state ζ. The spawned targets are not considered here. The PHD update equation is

$$\begin{aligned} D_{t|t}(x) =&(1 - p_D(x))D_{t|t-1}(x) \\ &+ \sum_{y \in Y_t} \frac{P_D(x)g_t(y|x)D_{t|t-1}(x)}{\kappa_t(y) + \int P_D(\zeta)g_t(y|\zeta)D_{t|t-1}(\zeta)d\zeta} \end{aligned} \quad (3)$$

where $P_D(\cdot)$ is the probability of detection and $\kappa_t(\cdot)$ denotes the intensity function of clutter at time t.

III. The framework for PF-PHD tracker

Our framework of biological micro-objects tracking typically consists of two stages (Fig. 1): microscopy image processing and micro-objects tracking based on the PF-PHD tracker. In the first stage, micro-objects of interest are detected separately in each image frame and their positions and shape parameters are extracted based on Mathematical morphology (MM). MM is proved to be a powerful tool for image analysis [27]. In our previous investigation, we mainly use MM to extract the shape parameters of micro-objects as measurement data in the latter tracking algorithm.

In the second stage we use the PF-PHD tracker to construct the trajectories of all detected micro-objects in the above stage. Since the PF-PHD tracker recursion accommodates complexities (such as the birth and death models) and embodies all available statistical information, it can be termed a complete solution to the estimation and tracking problem. In the PF-PHD tracker, PHD distribution evolves in the time and space domain, which is approximated by particles with weights. Then target states are estimated from the PHD distribution at each frame. According to the motion of micro-objects between frames, continuous trajectories are constructed according to the track continuity algorithm. For PF-PHD application, we present the ellipse target model to describe the shape information. Then a state evolution model is constructed to make better use of prior knowledge about the dynamics of micro-objects being tracked. In the tracking continuity stage, to deal

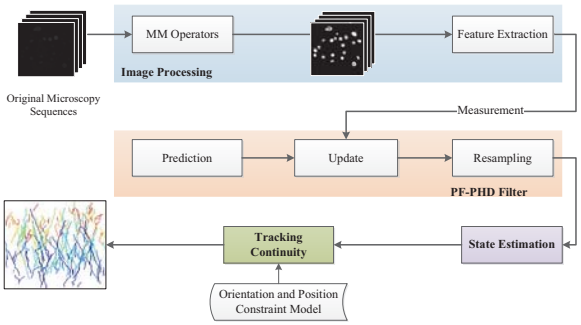

Fig. 1. Framework of the proposed tracking biological micro-objects method.

with the problems of the crossing trajectories, we model the orientational and positional constraints.

In the next, we give several models, including a state space model, PF-PHD trcker as well as the orientation and position constraints model to allow simultaneous tracking of multiple micro-objects crossing each other within this framework.

A. State Space Model

1) Target model: In many applications of biological micro-object tracking, the target is assumed to be visualised as a point superimposed on the background while the shape and structure are lost for a point target. In [6], Wood et al. used a GM-PHD filter to extract trajectories of free-swimming bacteria and they considered the bacteria as point-like targets without shape structure. This simplification reduced the complexity of tracking, but inevitably brought decline to tracking accuracy due to the lost information. Moreover, the study of dynamic properties requires the computation of parameters like shape, size, spatial distribution and orientation of the micro-objects. Therefore, point tracking can be made particularly inadequate in the context of microscopic video with shape. According to the shape and size of micro-objects in our biological scenarios, we consider the micro-object as an elliptic shape target instead of a point-like. Firstly, a definition of ellipse is given:

Definition 3.1: Ellipse. A two-dimensional ellipse with center c_t and positive-definite shape matrix A_t is given by the set $\{z|z \in \mathbb{R}^2 and (z-c_t)^T A_t^{-1}(z-c_t) \leq 1\}$ where

$$A_t = \begin{bmatrix} \cos\theta & -\sin\theta \\ \sin\theta & \cos\theta \end{bmatrix}^T \begin{bmatrix} a_t & 0 \\ 0 & b_t \end{bmatrix} \begin{bmatrix} \cos\theta & -\sin\theta \\ \sin\theta & \cos\theta \end{bmatrix} \quad (4)$$

and $\theta \in [-\pi/2, \pi/2)$ is the rotation angle between the X-axis and the major axis. $\begin{bmatrix} \cos\theta & -\sin\theta \\ \sin\theta & \cos\theta \end{bmatrix}$ is the rotation matrix. a_t, b_t are the length of the major and minor axes, respectively.

We represent the objects as ellipse with the state vector $\mathbf{x}_t = (x_t, \dot{x}_t, y_t, \dot{y}_t, a_t, b_t, \theta_t)$. Specifically, $(x_t, \dot{x}_t, y_t, \dot{y}_t) = \mathbf{v}_t$, where $(x_t, y_t) = \mathbf{r}_t$ is the center position of the ellipse target and $(\dot{x}_t, \dot{y}_t) = \dot{\mathbf{r}}_t$ is velocity. $(a_t, b_t, \theta_t) = \mathbf{s}_t$ is the object shape feature vector. Elliptical shapes are highly relevant for real biological applications since many mirco-objects, like some red blood cells, Escherichia coli, certain vesicles in the cytoplasm and Tanay virus from mosquitoes [28], can be considered approximately as an ellipsoid. Furthermore, elliptic shapes supply orientation information, which is quite useful in real world applications.

2) State evolution model : The dynamic state model is expressed in the following form:

$$\mathbf{x}_t = M\mathbf{x}_{t-1} + \xi \quad (5)$$

where $M = \mathtt{diag}(F, \mathbf{I}_3)$ is the sate transition matrix and $\xi \sim \mathcal{N}(\mathbf{0}, \mathtt{diag}(Q, Q_2))$ is the state noise where $\mathcal{N}(\mu, \Sigma)$ indicates the normal distribution with mean μ and covariance matrix Σ. Here we assume that state transition of $\mathbf{v}_t$ and shape feature vector $\mathbf{s}_t$ are independent. Therefore, our state evolution model $D_{\mathbf{x}_t|\mathbf{x}_{t-1}}$ can be factorized as

$$D_{\mathbf{x}_t|\mathbf{x}_{t-1}} = D_v(\mathbf{v}_t|\mathbf{v}_{t-1}) D_s(\mathbf{s}_t|\mathbf{s}_{t-1}). \quad (6)$$

Here $D_v(\mathbf{v}_t|\mathbf{v}_{t-1})$ is modeled using a linear Gaussian model

$$D_v(\mathbf{v}_t|\mathbf{v}_{t-1}) \propto e^{-\frac{1}{2}(\mathbf{v}_t - F\mathbf{v}_{t-1})^T Q^{-1}(\mathbf{v}_t - F\mathbf{v}_{t-1})} \quad (7)$$

with the process transition matrix F and covariance Q. Small changes in frame-to-frame micro-objects shape (appearance) are modeled using the Gaussian transition prior

$$D_s(\mathbf{s}_t|\mathbf{s}_{t-1}) = \mathcal{N}(\mathbf{s}_t|\mathbf{s}_{t-1}, Q_2) \quad (8)$$

where Q_2 represents the covariance matrix of target shape.

B. PF-PHD tracker

In order to implement the recursion (2) and (3), we use the PF-PHD tracker to interpret the prediction and update operators. The PF-PHD tracker is described as follows:

Step 1: Initialization. The shape parameters in the first image can be obtained as the prior knowledge to initialise the PF-PHD tracker.

Step 2: Prediction. At time $t \geq 2$, let $\{x_t^i, w_t^i\}$ denote a particle approximation of the PHD. For $i = 1, \ldots, L_{t-1}$, sample $\tilde{x}_t^i \sim q_t(\cdot|x_{t-1}^i, Y_t)$, which denotes the importance function of the particle filter. $\{\tilde{x}_t^i\}_{i=L_{t-1}+1}^{L_{t-1}+J_t}$ be J_t i.i.d samples from another proposal density $\pi_t(\cdot|Y_t)$, i.e.,

$$\tilde{x}_t^i \sim \begin{cases} q_t(\cdot|x_{t-1}^i, Y_t), \ i = 1, \ldots, L_{t-1} \\ \pi_t(\cdot|Y_t), \ i = L_{t-1}+1, \ldots, L_{t-1}+J_t \end{cases}$$

and the weights of particles

$$\tilde{w}_{t|t-1}^i \begin{cases} \frac{f_{t|t-1}(\tilde{x}_t^i, x_{t-1}^i)}{q_t(\tilde{x}_t^i|x_{t-1}^i, Y_t)} w_{t-1}^i, \ i = 1, \ldots, L_{t-1} \\ \frac{b_t(\tilde{x}_t^i)}{J_t \pi(\tilde{x}_t^i|Y_t)}, \ i = L_{t-1}+1, \ldots, L_{t-1}+J_t \end{cases}$$

Step 3: Update. For $i = 1, \ldots, L_{t-1} + J_t$, update weights $\tilde{w}_t^i = \left(1 - P_D(\tilde{x}_t^i) + \sum_{\mathbf{y}_j \in Y_t} G_t^{i,j}\right) \tilde{w}_{t|t-1}^i$ where $G_t^{i,j} = \frac{P_D L_t(\mathbf{y}_j|\tilde{x}_t^i)}{\kappa_t(\mathbf{y}_j) + C_t(\mathbf{y}_j)}$ and $C_t(\mathbf{y}_j) = \sum_{i=1}^{L_{t-1}+J_t} P_D L_t(\mathbf{y}_j|\tilde{x}_t^i) \tilde{w}_{t|t-1}^i$. Meanwhile, compute the sub-weight [29] of each particle for all observations $\mathbf{y}_j \in Y_t$, $\tilde{w}_t^{i,j} = G_t^{i,j} \tilde{w}_{t|t-1}^i$.

Step 4: Resampling. Compute the sum of particle weights $\hat{N}_{t|t} = \sum_{i=1}^{L_{t-1}+J_t} \tilde{w}_t^i$, then the expected number of targets $\hat{T}_t = round(\hat{N}_{t|t})$. Resampling $\{\tilde{x}_t^i, \frac{\tilde{w}_t^i}{\hat{N}_{t|t}}\}_{i=1}^{L_{t-1}+J_t}$ to get $\{x_t^i, w_t^i\}_{i=1}^{L_t}$, and the new weight of each particle is $\frac{\hat{N}_{t|t}}{L_t}$.

Step 5: State estimation. For each observation $\mathbf{y}_t^j$, $j = 1, \ldots, M_t$, compute the sum of sub-weights $W_t^j = \sum_{i=1}^{L_{t-1}+J_t} \tilde{w}_t^{i,j}$ relevant to $\mathbf{y}_t^j$. For $p = 1$ to $\hat{T}_t$, find the largest W_t^q, where $q = \arg_j \max(W_t^j)_{j=1}^{M_t}$. Return $\varsigma_t^p = w_t^{i,q} \cdot \tilde{x}_t^i$ as the pth estimated state, where $w_t^{i,q} = \frac{\tilde{w}_t^{i,q}}{\sum_{i=1}^{L_{t-1}+J_t} \tilde{w}_t^{i,q}}$ and let $W_t^q = 0$.

Step 6: Track Continuity. The track continuity mainly composes of three parts.

(1) computing weight matrix:

$$\begin{bmatrix} \tilde{w}_t^{l,1,1} & \tilde{w}_t^{l,1,2} & \ldots & \tilde{w}_t^{l,1,M_t} \\ \tilde{w}_t^{l,2,1} & \tilde{w}_t^{l,2,2} & \ldots & \tilde{w}_t^{l,2,M_t} \\ \ldots & \ldots & \ldots & \ldots \\ \tilde{w}_t^{l,M_{t-1},1} & \tilde{w}_t^{l,M_{t-1},2} & \ldots & \tilde{w}_t^{l,M_{t-1},M_t} \end{bmatrix}$$

where $\tilde{w}_t^{l,i,j} = \frac{P_D(\tilde{x}_t^l) L_t(\mathbf{y}_{t,j}|\tilde{x}_t^l) \tilde{w}_{t|t-1}^{l,i}}{\kappa_t(\mathbf{y}_{t,j}) + C_t(\mathbf{y}_{t,j})}$, $j = 1, \ldots, M_t$, $i = 1, \ldots, M_{t-1}$, $l = L_{t-1} + 1, \ldots, L_{t-1} + J_t$.

(2)Formulating association weight matrix:

$$W_A(t) = \begin{bmatrix} W_t^{1,1} & W_t^{1,2} & \ldots & W_t^{1,M_t} \\ W_t^{2,1} & W_t^{2,2} & \ldots & W_t^{2,M_t} \\ \ldots & \ldots & \ldots & \ldots \\ W_t^{M_{t-1},1} & \ldots & \ldots & W_t^{M_{t-1},M_t} \end{bmatrix}$$

where $W_t^{i,j} = \sum_{l=1}^{L_{t-1}+J_t} \tilde{w}_t^{l,i,j}$.

(3)Associating the target states. Search for the largest element $W_t^{p,q}$ in $W_A(t)$. If $W_t^{p,q}$ satisfies $W_t^{p,q} \geq W_{AH}$ (W_{AH} is a given threshold). If there is no less than one $W_t^{i,q} (i = 1, \ldots, M_{t-1})$ which also satisfies $W_t^{i,q} \geq W_{AH}$, use the state equation $\bar{\varsigma}_{t|t-1}^i = M\varsigma_{t-1}^i$ to predict their target states, and then select $\varsigma_{t-1}^{p'}$ with the least distance to ς_t^q by

$$p' = \arg_i \min_{W_t^{i,q} \geq W_{AH}} (\bar{\varsigma}_{t|t-1}^i - \varsigma_t^q)(\bar{\varsigma}_{t|t-1}^i - \varsigma_t^q)^T.$$

If there is no other $W_t^{i,q}$ satisfying $W_t^{p,q} \geq W_{AH}$, set $p' = p$. Put the estimated state pair $(\varsigma_{t-1}^{p'}, \varsigma_t^q)$ into the association set to indicate that state $\varsigma_{t-1}^{p'}$ and ς_t^q are originated from the same target. Then update $W_A(t)$ with $W_t^{p',j} = 0, j = 1, \ldots, M_t$; $W_t^{i,q} = 0, i = 1, \ldots, M_{t-1}$.

C. Track refinement

PHD filter may fail to distinguish the targets in very hard scenarios such as with many crossing targets [30]. For the crossing targets, particel labeling track continuity sometimes leads to identification inaccuracy or loss in the rough trajectories. We propose the orientation and position constraints model in PF-PHD tracker to tackle the problem of crossing trajectories. In our microscopy video, the movements of micro-objects are relatively steady and sudden turns or impropriety jumps hardly happen. Therefore, based on the assumption that there are limits of relative changes in position and orientation in two consecutive frames for one target, we confine the targets in the image sequences with a maximum length of positional moving d^* and a maximum angle of orientation moving θ^*.

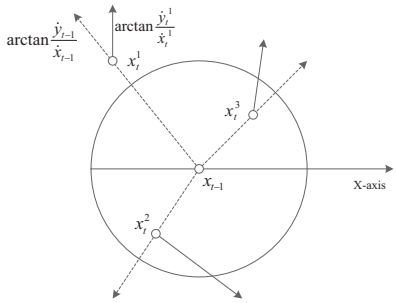

Fig. 2. Illustration of the constraint model

Proposition 3.1: Our orientation and position constraints model is in the following:

$$|x_{t-1,j} - x_{t,i}| \leq d_1^*, |y_{t-1,j} - y_{t,i}| \leq d_2^* \tag{9}$$

and

$$|\arctan \frac{\dot{y}_{t-1,j}}{\dot{x}_{t-1,j}} - \arctan \frac{\dot{y}_{t,i}}{\dot{x}_{t,i}}| \leq \theta^*. \tag{10}$$

If ($\mathbf{x}_{t-1}^j$, $\mathbf{x}_t^i$) is in the association set and satisfy the above constraint conditions, $\mathbf{x}_{t-1}^j$ and $\mathbf{x}_t^i$ are the same target and association pair ($\mathbf{x}_{t-1}^j$, $\mathbf{x}_t^i$) is accepted. In the constraint model, we confine the maximum motion of the target in a neighborhood whose central is $\mathbf{x}_{t-1}$ with radius $d^*(d_1^* = d_2^*)$ and the maximum moving orientation is θ^*. Fig. 2 shows the neighborhood of the constraint model. Here, we use $\arctan \frac{y_{t,j} - y_{t-1,i}}{x_{t,j} - x_{t-1,i}}$ to approximate $\arctan \frac{\dot{y}_{t-1}}{\dot{x}_{t-1}}$ and $d_1^* = d_2^* = d^*$ in Fig. 2. From Fig. 2, we find that $\mathbf{x}_t^1$ and $\mathbf{x}_t^2$ do not satisfy the constraint model due to $|y_{t-1} - y_{t,1}| > d_2^*$ and $|\arctan \frac{\dot{y}_{t-1}}{\dot{x}_{t-1}} - \arctan \frac{\dot{y}_{t,2}}{\dot{x}_{t,2}}| > \theta^*$. The motion from $\mathbf{x}_{t-1}$ to $\mathbf{x}_t^3$ is in the reasonable neighborhood, thus this trajectory satisfies the constraint model and it can be accepted. Under the confinements (9) and (10) the position of the micro-objects is constrained to lie within an appropriate distance, and their orientation at any given location is constrained to a reasonable angle against the wrong trajectory. Together, the constraint functions reduce the uncertainty of the state association.

Remark: Note that this constraint model is valid for the trajectories without a sudden turn or impropriety jump. If a trajectory has sharp changes or jump, the constraint model may bring out a wrong track association. However, there is a low probability of such events occurring in many biological applications.

IV. Experiment results

The experiment is testing on the simulated microtubule image sequences with a larger number of micro-objects ($50 - 70$ per frame). They are from an open competition at 2012 IEEE International Symposium on Biomedical Imaging [31]. There are 100 time frames of 512 $\times$ 512 pixels in the sequences.

1) Preprocessing of microscopy image sequences: Firstly, mathematical morphology (MM) is applied to enhance the original images and obtain the shape parameters. The original image for the first frame is shown in Fig. 3 (a). We apply

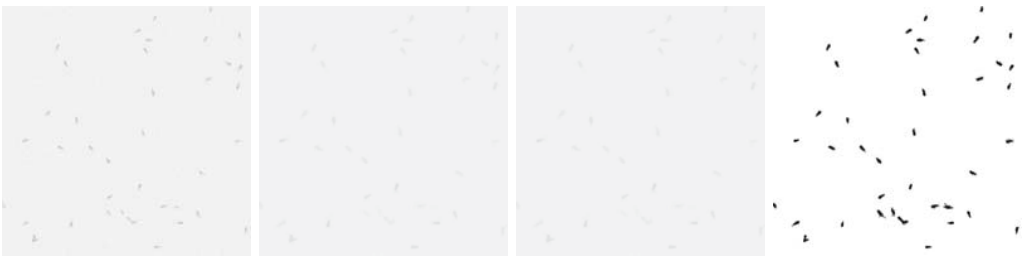

(a) (b) (c) (d)

Fig. 3. The preprocessed microscopy image based on mathematical morphological. (a) Original image. (b) Image after MM operators. (c) Opening-closing by morphological reconstruction. (d) Regional maxima of morphological reconstruction.

the basic MM operators to remove the noise in the original image that are represented as bright and dark values. The result is given in the Fig. 3 (b). Fig. 3 (c) shows the image by morphological reconstruction which combines opening-by-reconstruction operation and closing-by-reconstruction operation. In order to have better visibility, the regional maxima operator is applied to the processed image, and Fig. 3 (d) shows this result. From Fig. 3 (d), apparently, the white subregions are microtubules of interest.

2) Tracking initialization: In the PF-PHD trackers, the process transition matrix F in (7) is given $F = \mathtt{diag}(F_1, F_1)$ and covariance $Q = \mathtt{diag}(Q_1, Q_1)$ given by $F_1 = \begin{bmatrix} 1 & \Delta t \\ 0 & 1 \end{bmatrix}$ and $Q_1 = 60 \begin{bmatrix} \frac{1}{3}(\Delta t)^3 & \frac{1}{2}(\Delta t)^2 \\ \frac{1}{2}(\Delta t)^2 & \Delta t \end{bmatrix}$ where $\Delta t = 1s$.

The tracks are confined to a field of view of size 512×512 pixels. The new targets can appear at any location in the image. Thus the position of birth model is set to be a uniform density over the surveillance region $[0, 512] \times [0, 512]$, i.e., $b_t(\mathbf{r}_t) = \mathcal{U}(\mathbf{r}_t; [0, 512] \times [0, 512])$. The velocity and shape of new targets are modeled with intensity$b_t(\dot{\mathbf{r}}_t, \mathbf{s}_t) = \mathcal{N}(\dot{\mathbf{r}}_t, \mathbf{s}_t; m_b, P_b)$.

The initial number of particles is 4000 and the number of born particles for each new target is 300. In the orientation and position constraints model, the maximum moving bound for angle rotation is $\theta^* = 60°$ and the maximum length of position movement is $d_1^* = d_2^* = d^* = 20$ pixels. The tracking algorithm is programmed with Matlab code running on a 3.2 GHz Intel E5700 machine with 2G memory.

3) Experiment results: We compute the estimated target number, target state, and trajectories in order to evaluate the tracking performance of the proposed framework. The estimated number of targets (microtubule) is given in Fig. 4. The "true" number of targets is from careful manual identification. From Fig. 4, we find that the estimated number of targets has small errors compared with the manual identification except in the first frame (the first frame is used for initialization without number and state estimation). The number error primarily due to missing the observation at the image preprocess stage. The MM method failed to identify the corresponding micro-objects with low-contrast. Once the micro-objects are well detected at the image preprocess stage, the PF-PHD tracker will effectively track all the detected micro-objects. Fig. 5 (a) illustrates the state estimation for 4 consecutive frames and a detailed result is given in Fig. 5 (b) where the red curves

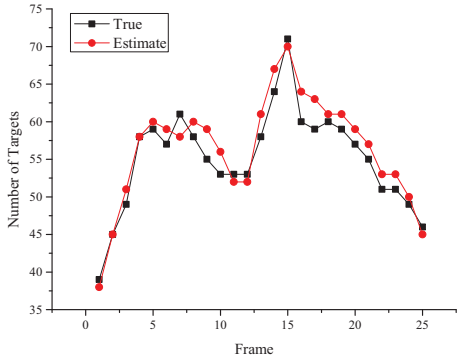

Fig. 4. The number of targets. The black square line is the number of targets from manual analysis and the red "o" line is the estimated number of targets of our approach.

are the boundary of micro-objects and the green ones are the estimated ellipses with yellow centers. From Fig. 5 (b), our method arrives at accurate state estimation with shape. Fig. 6 shows all trajectories in different frames (10, 15, 20, 25). The line linked to the target represents its trajectory before the current time step. If a trajectory disappears in the current frame, it is marked with a light grey line[1].

In order to verify the performance of the constraint models (9) and (10), a comparison of the trackers' effort was carried out on a selection of tracks with a careful manual analysis in Fig. 7. In Fig. 7 (a), the tracker output without the constraints model does not match up to the by-hand analysis and fails to track the crossing trajectories. The failure track was an incident where two targets moving to the same position are both simultaneously occluded by a third target as they cross. In Fig. 7 (b), the tracker output with the constraints model matches up to the manual tracking analysis and gives the three right crossing trajectories. Similar results in other scenarios show the effectiveness of the constraints model.

V. Conclusions

The micro-objects in microscopy video presents a challenge for automated tracking algorithms. PHD filter is a natural

[1]The track output for 100 frames is performed with a video in slow motion at http://sse.hit.edu.cn/wp-content/uploads/stepts100.rar

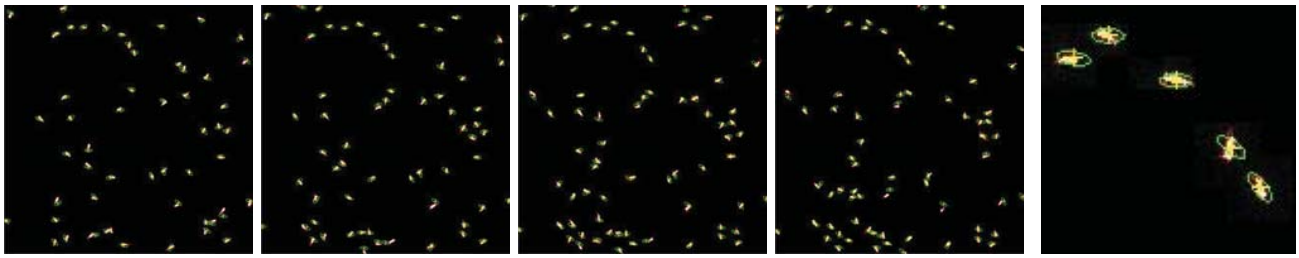

(a) The state estimation results for 11-14 frame

(b) Some detailed state estimation

Fig. 5. The state estimation results of four consecutive frames where the red points are the boundary of micro-objects and the green ellipses are the estimated targets with yellow "+"centers.

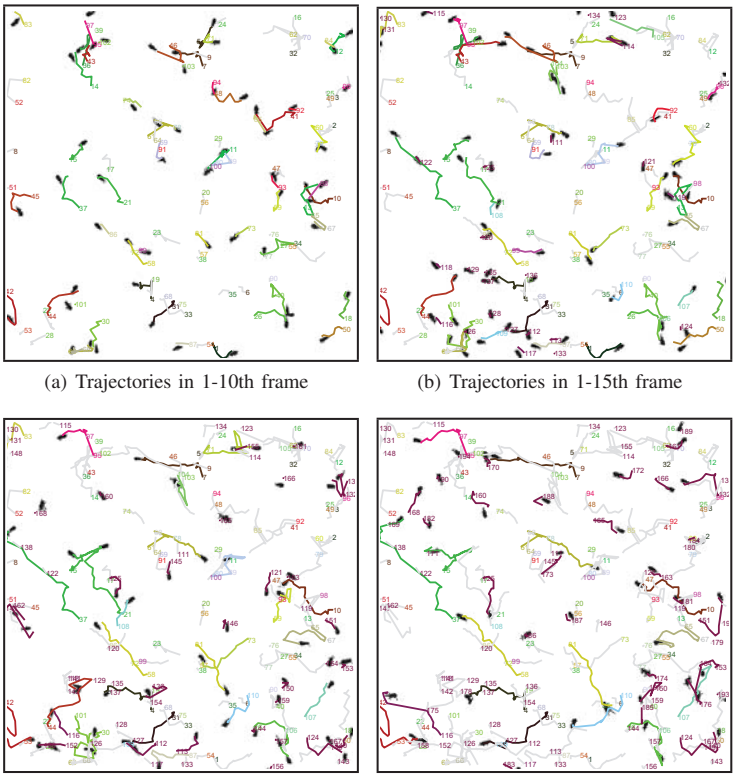

(a) Trajectories in 1-10th frame

(b) Trajectories in 1-15th frame

(c) Trajectories in 1-20th frame

(d) Trajectories in 1-25th frame

Fig. 6. The trajectories in different frame intervals.

solution to this problem due to its superior performance in dealing with the birth, spawn, and death of micro-objects as well as providing all available statistical information. We propose a PF-PHD tracking framework, which is an automated method capable of simultaneously tracking hundreds of micro-objects in the microscopy video. In the framework, we present a shape model to describe the elliptical micro-objects with kinds of orientation, size, and density instead of point-like targets. We further develop the orientational and positional constraints model (9) and (10) to deal with data association of crossing tracking. The results of experiments suggest that a significantly larger number of tracks are obtained and our PF-PHD tracker has an accurate state estimation with shape information. The PF-PHD tracker with constraint model can effectively tackle the crossing trajectories.

In some extreme biological conditions, MM is not sufficient for image preprocessing. Therefore, a better method of detecting objects with low-SNR or low-contrast is one of our future work. Meanwhile, we will continue to investigate the micro-object tracking method based on the Bayesian filter.

ACKNOWLEDGMENT

We would like to thank IEEE International Symposium on Biomedical Imaging (ISBI) for providing us the datasets.

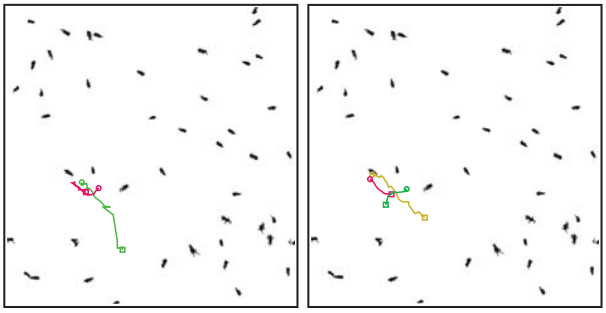

(a) Crossing trajectories without the constraint model

(b) Crossing trajectories with the constraint model

Fig. 7. Comparison of PF-PHD tracker without and with the orientation and position constraint model. The trajectories are indicated with "□"-locations at where targets are born and "○"-locations at where targets die.

This paper was supported by National Natural Science Foundation of China (NSFC) under Grant 61175027, 61305013 and the Research Fund for the Doctoral Program of Higher Education of China No.20132302120044 as well as the Fundamental Research Funds for the Central Universities No.HIT.NSRIF.2014071.

REFERENCES

[1] C. Zimmer, E. Labruyere, V. Meas-Yedid, N. Guillen, and J.-C. Olivo-Marin, "Segmentation and tracking of migrating cells in videomicroscopy with parametric active contours: A tool for cell-based drug testing," *Medical Imaging, IEEE Transactions on*, vol. 21, no. 10, pp. 1212–1221, 2002.

[2] D. McDonald, M. A. Vodicka, G. Lucero, T. M. Svitkina, G. G. Borisy, M. Emerman, and T. J. Hope, "Visualization of the intracellular behavior of hiv in living cells," *The Journal of cell biology*, vol. 159, no. 3, pp. 441–452, 2002.

[3] F. Frischknecht, P. Baldacci, B. Martin, C. Zimmer, S. Thiberge, and et al, "Imaging movement of malaria parasites during transmission by anopheles mosquitoes," *Cellular microbiology*, vol. 6, no. 7, pp. 687–694, 2004.

[4] A. Genovesio, T. Liedl, V. Emiliani, W. J. Parak, and other, "Multiple particle tracking in 3-d+ t microscopy: method and application to the tracking of endocytosed quantum dots," *Image Processing, IEEE Transactions on*, vol. 15, no. 5, pp. 1062–1070, 2006.

[5] L. Yuan, Y. F. Zheng, J. Zhu, L. Wang, and A. Brown, "Object tracking with particle filtering in fluorescence microscopy images: Application to the motion of neurofilaments in axons," *Medical Imaging, IEEE Transactions on*, vol. 31, no. 1, pp. 117–130, 2012.

[6] T. M. Wood, C. A. Yates, D. A. Wilkinson, and G. Rosser, "Simplified multitarget tracking using the phd filter for microscopic video data," *Circuits and Systems for Video Technology, IEEE Transactions on*, vol. 22, no. 5, pp. 702–713, 2012.

[7] A. Yilmaz, O. Javed, and M. Shah, "Object tracking: A survey," *Acm computing surveys (CSUR)*, vol. 38, no. 4, p. 13, 2006.

[8] K. Miura, "Tracking movement in cell biology," in *Microscopy Techniques*. Springer, 2005, pp. 267–295.

[9] E. Meijering, O. Dzyubachyk, I. Smal *et al.*, "Methods for cell and particle tracking," *Methods Enzymol*, vol. 504, no. 9, pp. 183–200, 2012.

[10] K. Schindler, "Continuous energy minimization for multi-target tracking," *Pattern Analysis and Machine Intelligence, IEEE Transactions on*, vol. 36, no. 1, 2014.

[11] D. P. Mukherjee, N. Ray, and S. T. Acton, "Level set analysis for leukocyte detection and tracking," *Image Processing, IEEE Transactions on*, vol. 13, no. 4, pp. 562–572, 2004.

[12] F. Yang, M. A. Mackey, F. Ianzini, G. Gallardo, and M. Sonka, "Cell segmentation, tracking, and mitosis detection using temporal context," in *Medical Image Computing and Computer-Assisted Intervention–MICCAI 2005*. Springer, 2005, pp. 302–309.

[13] N. Paragios and R. Deriche, "Geodesic active contours and level sets for the detection and tracking of moving objects," *Pattern Analysis and Machine Intelligence, IEEE Transactions on*, vol. 22, no. 3, pp. 266–280, 2000.

[14] H. Geerts, M. De Brabander, R. Nuydens, S. Geuens, and other, "Nanovid tracking: a new automatic method for the study of mobility in living cells based on colloidal gold and video microscopy," *Biophysical journal*, vol. 52, no. 5, pp. 775–782, 1987.

[15] C. J. Veenman, M. J. Reinders, and E. Backer, "Motion tracking as a constrained optimization problem," *Pattern Recognition*, vol. 36, no. 9, pp. 2049–2067, 2003.

[16] S. Bonneau, M. Dahan, and L. D. Cohen, "Single quantum dot tracking based on perceptual grouping using minimal paths in a spatiotemporal volume," *Image Processing, IEEE Transactions on*, vol. 14, no. 9, pp. 1384–1395, 2005.

[17] L. Zhang, Y. Li, and R. Nevatia, "Global data association for multi-object tracking using network flows," in *Computer Vision and Pattern Recognition, 2008. CVPR 2008. IEEE Conference on*. IEEE, 2008, pp. 1–8.

[18] R. Chatterjee, M. Ghosh, A. S. Chowdhury, and N. Ray, "Cell tracking in microscopic video using matching and linking of bipartite graphs," *Computer methods and programs in biomedicine*, vol. 112, no. 3, pp. 422–431, 2013.

[19] N. Chenouard, I. Bloch, and J.-C. Olivo-Marin, "Multiple hypothesis tracking in microscopy images," in *Biomedical Imaging: From Nano to Macro, 2009. ISBI'09. IEEE International Symposium on*. IEEE, 2009, pp. 1346–1349.

[20] I. Smal, W. Niessen, and E. Meijering, "A new detection scheme for multiple object tracking in fluorescence microscopy by joint probabilistic data association filtering," in *Biomedical Imaging: 5th IEEE International Symposium on*. IEEE, 2008, pp. 264–267.

[21] K. Jaqaman, D. Loerke, M. Mettlen, H. Kuwata, S. Grinstein, S. L. Schmid, and G. Danuser, "Robust single-particle tracking in live-cell time-lapse sequences," *Nature methods*, vol. 5, no. 8, pp. 695–702, 2008.

[22] R. P. Mahler, "Multitarget bayes filtering via first-order multitarget moments," *Aerospace and Electronic Systems, IEEE Transactions on*, vol. 39, no. 4, pp. 1152–1178, 2003.

[23] E. Maggio, M. Taj, and A. Cavallaro, "Efficient multitarget visual tracking using random finite sets," *Circuits and Systems for Video Technology, IEEE Transactions on*, vol. 18, no. 8, pp. 1016–1027, 2008.

[24] Y.-D. Wang, J.-K. Wu, A. A. Kassim, and W. Huang, "Data-driven probability hypothesis density filter for visual tracking," *Circuits and Systems for Video Technology, IEEE Transactions on*, vol. 18, no. 8, pp. 1085–1095, 2008.

[25] R. P. Mahler, *Statistical multisource-multitarget information fusion*. Artech House Norwood, 2007, vol. 685.

[26] B.-N. Vo, S. Singh, and A. Doucet, "Sequential monte carlo methods for multitarget filtering with random finite sets," *Aerospace and Electronic Systems, IEEE Transactions on*, vol. 41, no. 4, pp. 1224–1245, 2005.

[27] Y. Kimori, "Mathematical morphology-based approach to the enhancement of morphological features in medical images," *Journal of clinical bioinformatics*, vol. 1, no. 1, pp. 1–10, 2011.

[28] T. Nabeshima, S. Inoue, K. Okamoto, G. Posadas-Herrera, F. Yu *et al.*, "Tanay virus, a new species of virus isolated from mosquitoes in the philippines," *Journal of General Virology*, vol. 95, no. Pt 6, pp. 1390–1395, 2014.

[29] L. Zhao, P. Ma, X. Su, and H. Zhang, "A new multi-target state estimation algorithm for phd particle filter," in *Information Fusion (FUSION), 2010 13th Conference on*. IEEE, 2010, pp. 1–8.

[30] K. Panta, D. E. Clark, and B.-N. Vo, "Data association and track management for the gaussian mixture probability hypothesis density filter," *Aerospace and Electronic Systems, IEEE Transactions on*, vol. 45, no. 3, pp. 1003–1016, 2009.

[31] N. Chenouard, I. Smal, F. De Chaumont, M. Maška *et al.*, "Objective comparison of particle tracking methods," *Nature methods*, 2014.